

# Optimal Design of Induction Heater considering Magnetic Skin Effect

Byoung-Wook Jo, Byeong-Chul Lee, Cheon-Ho Song, Ki-Chan Kim

*Positive temperature coefficient (PTC) heaters are currently used for heating the batteries of electric vehicle(EV)s. However, PTC heaters have a problem of fire safety from mal-function. Induction heater is a good candidate for safety and cost. It is operated in the high frequency range above 20 kHz. The work piece (WP) of the induction heater has a magnetic field concentrated only on the surface due to the magnetic skin effect at high frequency. Skin Effect in WP makes the reluctance of magnetic circuit increase and makes inductance and core loss decrease. In this paper, an optimum design of the induction heater is proposed by finite element method (FEM) simulation. As a result of FEM analysis, the inductance and the core loss of induction heater are the highest as the magnetic material of WP is replaced with the ferrimagnetic materials without being influenced by the magnetic skin effect. As a result of the optimization design and comparison study, the optimization model shows that core loss occurring on the outside WP generates more than the sum of the inner and outer parts of the base model. The inductance increased by 2.18 times and the iron loss by 1.83 times.*

*Index Terms: Core loss, Ferrimagnetic material, Inductance, Induction heater, Magnetic skin effect*

## I. INTRODUCTION

Research and development of electric vehicle(EV)s is active due to environmental pollution regulations. A lithium ion battery is used to drive a motor of EVs. If the lithium ion battery is not maintained at an appropriate temperature, A lithium ion battery efficiency is deteriorated. Currently, PTC heaters are used for lithium ion battery and indoor heating in EVs. PTC heaters are a heater used in conventional hybrid cars. However, PTC heaters are not a suitable heating system of EVs in that EVs cannot be used for the waste heat of the internal combustion engine. Also, PTC heaters have a problem of fire safety from mal-function. On the other hand, the induction heater is light in weight due to the simple insulation package, and can maintain the proper temperature of the battery within a short time due to the rapid temperature rise characteristics, thereby improving the one charge traveling distance of EVs[1].

In the induction heater, the heating element is called the work piece(WP). The WP of the induction heater is a ferromagnetic material capable of generating high core loss. Since the hysteresis loss is proportional to the frequency, the eddy current loss is proportional to square the frequency, and the excess loss is proportional to 1.5 times the frequency, among the core loss, the induction heater is typically operated in the high frequency range above 20 kHz[2]-[5]. In the high frequency region, the magnetic field is concentrated only on the surface due to the magnetic skin effect, and the

inductance is decreased due to the increase of the reluctance[6]-[9]. The induction heater is composed of a series LC resonant circuit and the capacitance increases as the inductance drops This phenomenon is not desirable because the capacitance is proportional to price and weight[10]. This paper, an optimum design of the inductance and core loss of the induction heater using ferrite magnetic material is proposed through finite element method (FEM) simulation.

## II. INDUCTION HEATER ANALYSIS

### A. Analysis Model of Induction Heater

Fig. 1 and Table 1 show the 2D FEM simulation base model and specifications of the induction heater, respectively. As shown in Fig. 1, the induction heater generally has a simple structure composed of the inner and outer WP, an external shielding material, and a coil generating magnetomotive force (MMF). In addition, the coil used the litz wire twisted in several strands to reduce the skin effect and proximity effect. The SUS430F, which is a ferromagnetic material, was selected as the WP, and shielding material is a conductor favoring high frequency shielding material. As shown in Table 1, The specifications of litz wire are 1.97 mm in coil diameter, 200 in the number of reels, and 0.1 mm in reel diameter. The thickness of the WP was made thin with a thickness of 1 mm because the magnetic field concentrates only on the surface due to the magnetic skin effect.

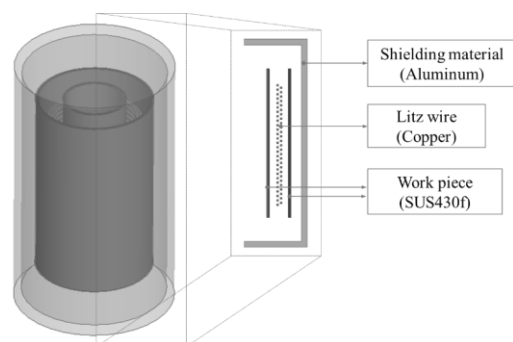


Fig. 1. 2D FEM simulation base model of the induction heater

Table I. Specifications of the induction heater

Spec.		Value	Unit
WP	Inner dia.	33.3	mm
	Outer dia.	62.1	mm
	Inner thickness	1	mm
	Outer thickness	1	mm
	Inner height	100	mm
	Outer height	100	mm
Litz wire	Coil dia	1.97	mm
	The num of reels	200	-
	Reel dia	0.1	mm
Shielding material	Heigh	140	mm

**B.LC Resonance Circuit**

Fig. 2 shows LC resonance circuit and characteristic of the induction heater according to the frequency. As shown in Fig. 2, the induction heater is driven at the resonant frequency by the LC resonant circuit. The inductance of the induction heater and the capacitor connected in a series with the coil, and the reactance can be minimized to maximize the input power at the resonance frequency. The input power of the induction heater is mostly converted to heat and generated as an output. The resonance frequency is calculated as show in (1). The capacitance must increase as the inductance decreases. Since the capacitance is proportional to price and weight, it is advantageous to increase the inductance and lower the capacitance.

$$f_r = \frac{1}{2\pi\sqrt{LC}} \tag{1}$$

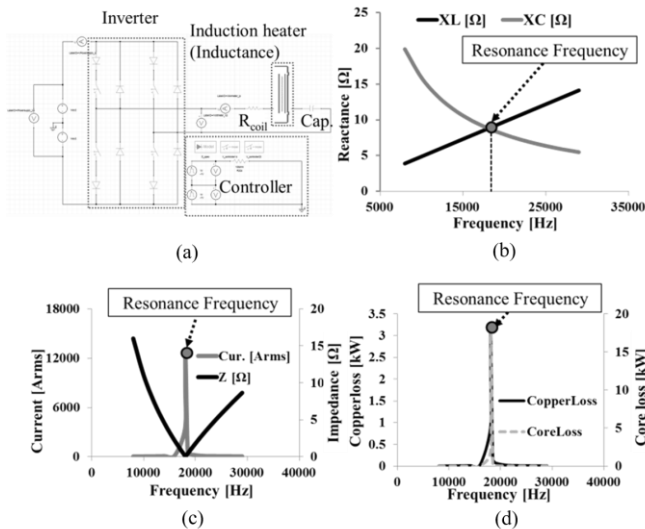


Fig. 2. LC resonance circuit and Characteristics of induction heater according to the frequency (a) LC resonance circuit (b) Reactance according to the frequency (c) Current and impedance according to the frequency (d) Copperloss and coreloss according to the frequency

**C.Magnetic equivalent circuit**

Figure 3 shows the magnetic equivalent circuit of the induction heater. Equation (2), (3), and (4) show respectively reluctance, depth of penetration, and total flux.

$$\mathfrak{R} = \frac{l}{\mu S} \tag{2}$$

$$\delta = \frac{1}{\sqrt{\pi f \mu \sigma}} \tag{3}$$

$$\phi = \frac{Ni}{\mathfrak{R}_{Inner,WP} + \mathfrak{R}_{Top,Air} + \mathfrak{R}_{Bottom,Air} + \mathfrak{R}_{Inner,WP}} \tag{4}$$

where  $l$ ,  $\mu$ ,  $S$ ,  $f$ ,  $\sigma$ ,  $\phi$ , and  $Ni$  is respectively length of flux linkage, permeability, area where magnetic flux is interlinked, operating frequency, conductivity, and MMF. The induction heater is converted from electric energy to magnetic energy, and this magnetic energy is converted into thermal energy which is the sum of the core loss and copper loss. Thermal energy is almost the core loss. Therefore, the total flux must be increased to decrease reluctance of the inner or outer WP.

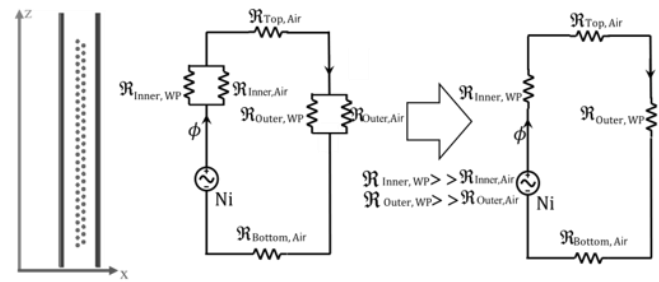


Fig. 3. The magnetic equivalent circuit of the induction heater

**D. Optimization considering magnetic skin effect**

Figure 4 show flux density distribution of the induction heater. As shown in Figure 4, the WP is a ferromagnetic material, which has a high conductivity and high permeability, so that the depth of penetration is small, which limits the reduction of reluctance by the thickness of the WP. That is, there is a limit to increase the total magnetic flux by thickness change of the WP.

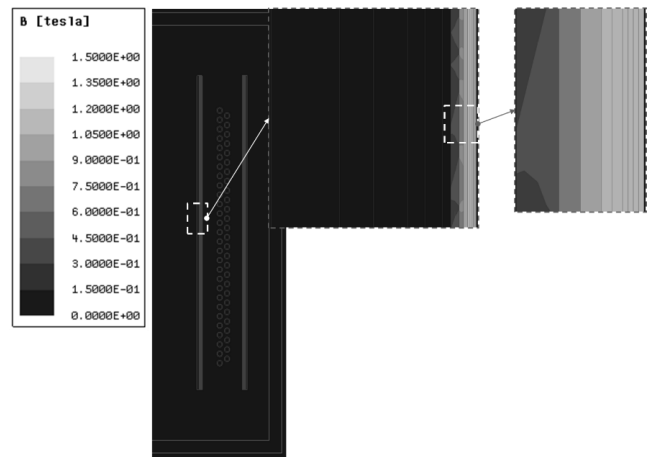


Fig. 4. Flux density distribution of the induction heater

Figure 5 show models of the induction heater. Base model represents both the inner material and outer material are SUS430. Model A represents the inner material and the outer material are



respectively sendust and SUS430. Model B represents the inner material and the outer material are respectively SUS430 and sendust. SUS430 and sendust are respectively a ferromagnetic material and a ferrimagnetic material. Base model, model A, and the model B increase respectively the thickness of the inner material to the inside and the outer material to the outside to see exactly how much the total flux increases by changing the inner and the outer magnetic material in that the air gap reluctance is not changed. Also, model A and model B replace the one of the two WP with a ferrimagnetic material instead of a ferromagnetic material since a ferrimagnetic material is that its conductivity is low, the depth of penetration is high even at high frequency.

Figure 6 show characteristics of the base model according to inner and outer WP thickness. Figure 6 is the result obtained at  $I_{rms}=18$  A and RL circuit. As can be seen from Figure 6, when the WP is under 0.6 mm, since the magnetic field is less influenced by the magnetic skin effect, the reluctance is reduced, and the total flux increases. As the WP is 0.6 mm or more, the inductance and core loss are kept constant due to the magnetic skin effect.

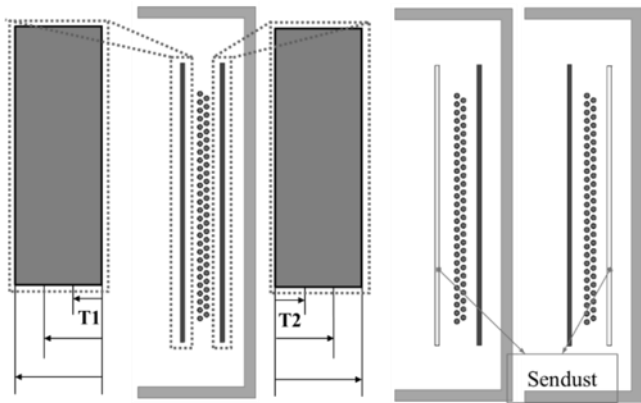


Fig. 5. Models of the induction heater (a) Base model (b) Model A (c) Model B

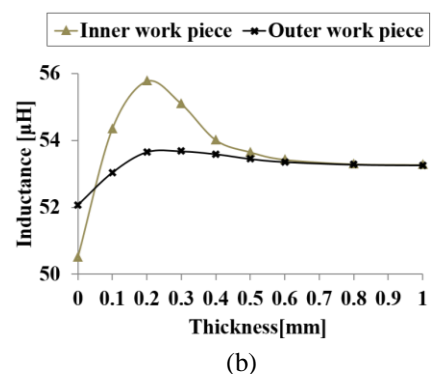
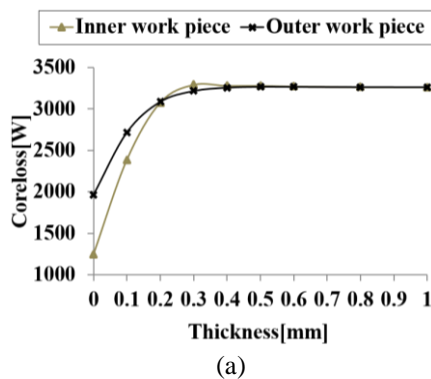


Fig. 6. The characteristics of the base model according to inner and outer WP thickness (RL circuit  $I_{rms}=18$  A) (a) Core loss (b) inductance

Figure 7 shows characteristics of model A and model B according to thickness. Both model A and model B are the result obtained at  $I_{rms}=18$  A and RL circuit. Also, model A is a thickness change of the inner sendust and model B is a thickness change of the outer sendust. As can be seen from Figure 7, it is found that because the reluctance is reduced, the total flux increase, the inductance and core loss increase without being influenced by the magnetic skin effect. However, the rate of increase decreases steadily due to the saturation of the BH curve. Also, it can be seen that the core loss and inductance are higher when the sendust is used inside rather than outside. Equation (5) show the inductance. As can be seen from (5), the inductance is the largest when the flux is linked to all the coils if the flux is the same. Also, the flux is concentrated toward the lower reluctance. For the above reasons, the model B has a small reluctance outside the coil, which concentrates the flux. Therefore, the model B has a smaller the inductance and core loss due to a large number of fluxes that cannot be linked to all coil than the model A. For the above reasons, the optimization model is model A, a thickness of sendust is 2 mm, and a thickness of the SUS430 is 1 mm.

$$\lambda = \frac{N\phi}{I} \quad (5)$$

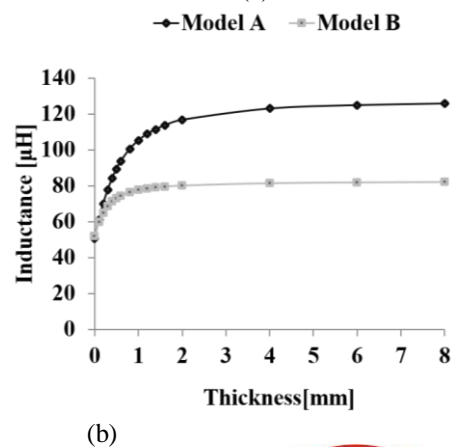
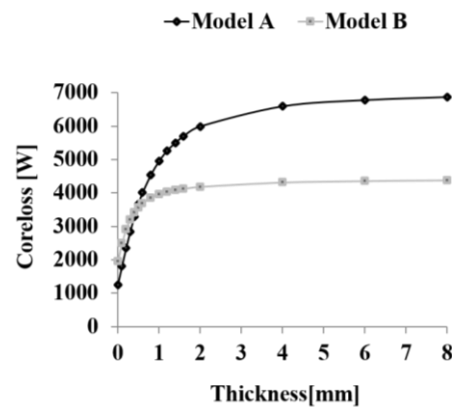


Fig. 7. The characteristics of the model A and model B according to inner and outer WP thickness (RL circuit  $I_{rms}=18$  A) (a) Core loss (b) inductance



inductance

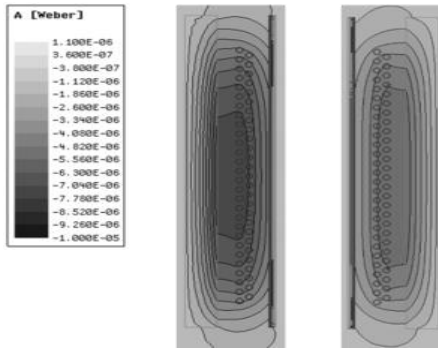


Fig. 8. The characteristics of the base model according to inner and outer WP thickness (RL circuit  $I_{rms}=18$  A) (a) Coreloss (b) inductance

Table II. Comparison of optimization model and base model

	Base model	Optimization model	Unit
Inductance	53.26	116.63	$\mu\text{H}$
Core loss	3263.81	5997.92	W

### III. CONCLUSION

In this paper, the optimization design is studied by changing the material and thickness of the inner and outer magnetic materials considering the magnetic skin effect of the induction heater for EVs. As a result, when inner and outer magnetic materials were used only with ferromagnetic material, the inner and outer magnetic materials were disadvantageous in terms of magnetic circuit due to magnetic skin effect, and the inductance and core loss were lowest. The inductance and the core loss were the highest when the magnetic material was replaced with the ferrimagnetic material in the inside without being influenced by the magnetic skin effect. The results of Figure 9 and Table 2 are derived through FEM simulation. As shown in Fig. 9, the optimization model shows that the inner material does not generate heat, but the core loss occurring on the outside generates more amount than the sum of the inner and outer parts of the base model. In addition, as shown in Table 2, the inductance increased by 2.18 times and the iron loss by 1.83 times. Therefore, it is better to use the inner ferrimagnetic material of the induction heater.

### ACKNOWLEDGMENT

This work was supported by the Technology Innovation Program (10070181, 6 kW Integrated Induction Coolant Heater System Development for Battery and Cabin Heating) funded by the Ministry of Trade, Industry and Energy (MI, South Korea).

### REFERENCES

1. A. Boadi, Y. Tsuchida, T. Todaka, and M. Enokizono, "Designing of suitable construction of high-frequency induction heating coil by using finite-element method," *IEEE Transaction on Manetics.*, vol.41, Oct. 2005, pp. 4048-4050.

2. P. Urbanek, A. Skorek, and M. B. Zaremba, "Magnetic flux and temperature analysis in induction heated steel cylinder," *IEEE Transactions on Magnetics.*, vol. 30, Sep. 1994, pp. 3328-3330.

3. P. Dorland, J. D. van Wyk, and O. H. Stielau, "On the influence of coil design and electromagnetic configuration on the efficiency of an induction melting furnace," *IEEE Transactions on Industry Applications.*, vol. 36, Jul. / Aug. 2000, pp. 946-957.

4. Nikolaos Tsopelas, and Nikolaos J. Siakavellas, "Influence of Some Parameters on the Effectiveness of Induction Heating," *IEEE Transactions on Magnetics.*, vol. 44, Dec. 2008, pp. 4711-4720.

5. Acero J, Carretero C, Alonso R and Burdio J.M, "Quantitative Evaluation of Induction Efficiency in Domestic Induction Heating Applications," *IEEE Transactions on Magnetics.*, vol. 49, Apr. 2013, pp. 1382-1389.

6. M. Enokizono, T. Todaka, and S. Nishimura, "Finite element analysis of high-frequency induction heating problems considering inhomogeneous flow of exciting currents," *IEEE Transactions on Magnetics.*, vol. 35, May. 1999, pp. 1646-1649.

7. S. M. Jang, S. K. Cho, S.-H. Lee, H. W. Cho, and H. C. Park, "Thermal analysis of induction heating roll with heat pipes," *IEEE Transactions on Magnetics.*, vol. 39, Sep. 2003, pp. 3244-3246.

8. Z. Keyi, L. Bin, L. Zhiyuan, C. Shukang, and Z. Ruiping, "Inductance computation consideration of induction coil launcher," *IEEE Transactions on Magnetics.*, vol. 45, Jan. 2009, pp. 336-340.

9. Weimin Cuan, Di Zhang, Yiyang Zhu, Yanhui Gao, and Kzauhiro Muramatsu, "Numerical Modeling of Iron Loss Considering Laminated Structure and Excess Loss," *IEEE Transactions on Magnetics.*, vol. 54, Nov. 2018.

10. José M. Espí Huerta, Enrique J. Dede García Santamaría, Rafael García Gil, and Jaime Castelló Moreno, "Design of the L-LC Resonant Inverter for Induction Heating Based on Its Equivalent SRI," *IEEE Transactions on Industrial Electronics.*, vol. 54, Nov. 2007, pp. 3178-3187

### AUTHORS PROFILE



**Byong-Wook Jo** He received B.S degree in electrical engineering from Hanbat National University, Daejeon, Korea in 2018. Since 2018, he is in course of M.S. degree from Hanbat National University. His research interests are design and analysis of electrical machinery.



**Byung-Chul Lee** He received B.S degree in electrical engineering from Hanbat National University, Daejeon, Korea in 2019. Since 2019, he is in course of M.S. degree from Hanbat National University. His research interests are design and analysis of electrical machinery.



**Cheon-Ho Song** He received B.S degree in electrical engineering from Hanbat National University, Daejeon, Korea in 2019. Since 2019, he is in course of M.S. degree from Hanbat National University. His research interests are design and analysis of electrical machinery.



**Ki-Chan Kim** He received the B.S. and M.S. degrees all in electrical engineering from Hanyang University, Seoul, Korea, in 1996 and 1998, respectively. From 1998 to 2004, he was a research engineer at the Electro-Mechanical Research Institute of Hyundai Heavy Industries Co., LTD. He received the Ph. D degrees in electrical engineering from Hanyang University, Seoul, Korea, in 2008. Since 2005, he is professor in the Department of Electrical Engineering, Hanbat National University. His research interests include design, analysis, testing and control of motors, generators and electromagnetic sensors for electric vehicle, trains and wind turbine.

